

Influence of step-induced anti-phase boundaries on the surface morphology of zincblende-type semiconductors

Z. H. CHEN(*), M. SOKOLOWSKI(**), F. STADLER,
M. SCHNEIDER, R. FINK and E. UMBACH

*Experimentelle Physik II, Universität Würzburg
Am Hubland, Würzburg, D-97074, Germany*

(received 25 July 2001; accepted in final form 30 May 2002)

PACS. 68.35.Bs – Structure of clean surfaces (reconstruction).

PACS. 61.14.Hg – Low-energy electron diffraction (LEED) and reflection high-energy electron diffraction (RHEED).

Abstract. – Using high-resolution low-energy electron diffraction, we find a “correlation” of the $c(2 \times 2)$ reconstruction of the ZnSe(001) surface *across* [010]- and [100]-oriented steps. The difference of the corresponding step vectors is incompatible with the $c(2 \times 2)$ reconstruction. Thus intersection points of [010]- and [100]-oriented steps at 2D island corners or kinks induce $c(2 \times 2)$ anti-phase boundaries along the $[1\bar{1}0]$ direction. This mechanism yields a *non-local* contribution to the step energy which generally could be important for the explanation of step morphologies, *e.g.*, of the recently observed, self-organized checkerboard-like arrangement of nano-terraces on a vicinal CdTe(001) surface.

Surface morphologies on the nanometer scale are largely determined by the properties of steps of atomic height. Especially for surfaces of diamond or zincblende-type semiconductors, theoretical and experimental efforts have been made to understand surface steps on an atomic scale, as well as the step evolution during growth processes [1–4]. An important aspect in this context is the relation of steps and surface reconstructions. For instance, on the Si(001) surface the elongated shape of (2×1) or (1×2) reconstructed islands is related to the high sticking probability for Si atoms at the ends of the Si dimer rows [4], and similarly, for the steps on the polar GaAs(001) surface a strong preference of steps running along the (2×1) reconstructed direction exists [5]. In both cases, the surface reconstruction (superstructure) is decisive for the local energy (line tension) of the steps and determines, possibly in combination with kinetic effects, the step morphology.

In this letter we address a novel aspect. Based on a particular example, the $c(2 \times 2)$ reconstructed polar ZnSe(001) surface, we describe a situation, where the *interaction between steps*

(*) On leave from National Laboratory of Infrared Physics, Shanghai Institute of Technical Physics, Chinese Academia Sinica - Shanghai, 200083, PRC.

(**) Present address: Institut für Physikalische und Theoretische Chemie der Universität Bonn - Wegelerstr. 12, D-53115 Bonn, Germany. E-mail: sokolowski@thch.uni-bonn.de

is mediated by the superstructure and influences the *global step morphology*. This interaction is related to anti-phase domain boundaries that we find to emerge at step intersection points, which are present on surfaces, *e.g.*, at 2D island corners or kinks. Such anti-phase boundaries are energetically unfavorable and will thus be minimized, leading to a mutual “attraction” of kinks and corners. We investigated this situation in detail for the ZnSe(001) surface by using high-resolution low-energy electron diffraction (SPA-LEED). However, this situation is expected for other polar II-VI semiconductor surfaces, too, and may be important—in a modified form—also for a large range of other reconstructed surfaces.

For the $c(2 \times 2)$ superstructure of ZnSe(001), a surface reconstruction with half a monolayer of Zn (Zn-vacancy model, see fig. 3, below) is expected on the basis of theoretical calculations [6] and supported by photoemission experiments [7, 8]. Recent reflection-high-energy-electron-diffraction results suggested a Se-vacancy model [9]. However, very recent X-ray diffraction experiments confirm the Zn-vacancy model unambiguously [10]. For the conclusions drawn in this paper the exact details of $c(2 \times 2)$ surface reconstruction are not relevant.

The reported experiments were performed on *p*-doped molecular-beam-epitaxial (MBE) grown ZnSe layers (approximately $1 \mu\text{m}$ thick) on *p*-type, nominally flat GaAs (001) substrates. Clean Zn-terminated $c(2 \times 2)$ -reconstructed ZnSe(001) surfaces, as monitored by X-ray photoelectron spectroscopy and SPA-LEED [8], were prepared by several *in situ* cycles of sputtering with 1 keV Ar^+ ions ($5 \mu\text{A}/\text{cm}^2$, ~ 5 min) and subsequent annealing at 400°C for about 20 min in ultrahigh vacuum.

1D and 2D SPA-LEED data were measured at room temperature for various electron energies. Figure 1 displays LEED patterns for two energies corresponding to the in-phase and anti-phase condition of the central (0, 0) spot, respectively. This condition arises from the relative phase difference φ between electron waves scattered from two domains on the surface separated by one step (but which are otherwise identical). It is given by the step vector \mathbf{g} and the scattering vector \mathbf{k} ($\mathbf{k} = \mathbf{k}_{\text{final}} - \mathbf{k}_{\text{initial}}$) [11]:

$$\varphi = \mathbf{g} \cdot \mathbf{k} = \mathbf{g}_\perp \cdot \mathbf{k}_\perp + \mathbf{g}_\parallel \cdot \mathbf{k}_\parallel, \quad (1)$$

where \perp and \parallel denote the components perpendicular and parallel to the surface. A step vector \mathbf{g} is understood as a vector that allows to map any two surface unit cells on two adjacent terraces onto each other by $\mathbf{g} + \mathbf{v}$, \mathbf{v} being a translational vector of the ideal reconstructed 2D surface [11, 12]. Since the variation of the electron energy leads to a variation of \mathbf{k}_\perp and consequently of φ , *constructive* (in-phase) and *destructive* (anti-phase) interference conditions alternate with energy.

In figs. 1(a) and (b), the first-order $c(2 \times 2)$ superstructure spots ($\pm\frac{1}{2}, \pm\frac{1}{2}$) are clearly visible in addition to the (1×1) spots of the ZnSe(001) surface. This demonstrates that a well-ordered $c(2 \times 2)$ surface reconstruction is achieved by the chosen preparation. The next interesting finding from figs. 1(a) and (b) is that the central specular (0, 0) spot is sharp at 75 eV (in-phase condition), but broadened with a fourfold symmetry along the [010] and [100] directions at 57 eV electron energy (anti-phase condition). This clearly reveals that the surface exhibits a significant concentration of steps. From an analysis of the variation of the full width of half-maximum (FWHM) (along the [010] and [100] directions) of the (0, 0) spot as a function of \mathbf{k}_\perp we determined the in- and anti-phase conditions. Using eq. (1), a step height ($|\mathbf{g}_\perp|$) of $a/2$ ($a = 5.67 \text{ \AA}$) is found, which exactly corresponds to the spacing between subsequent Zn or Se layers [8]. This implies that a large majority of the terraces on the surface must exhibit the same termination. Since one unique superstructure is observed in LEED, the *same* reconstruction must be present on all terraces.

From the fact that the broadening of the (0, 0) spot is preferentially in the [010] and [100] directions (see fig. 1(b)), one can further deduce that the steps are preferentially parallel

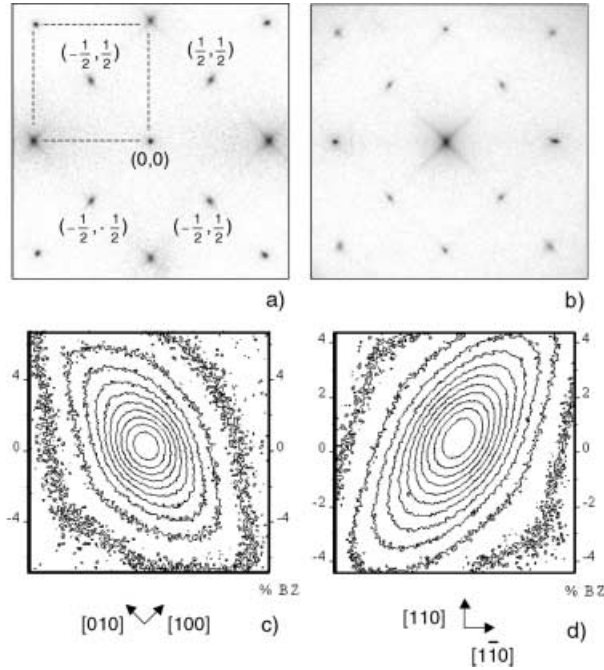


Fig. 1 – SPA-LEED patterns of the sputter-annealed ZnSe(001)- $c(2 \times 2)$ surface at (a) 75 eV, and (b) 57 eV electron energy, corresponding to the *in-phase* and *anti-phase* conditions of the (0, 0) spot, respectively. The dashed square indicates the (1×1) unit cell. The panels (c) and (d) show the $(\frac{1}{2}, -\frac{1}{2})$ spot on an enlarged scale at these two energies. The width of the box is about 10% of the surface Brillouin zone (BZ).

to each other and oriented perpendicular to the directions of the broadening, *i.e.* along the [100] and [010] directions (see fig. 3 below). Steps running along these directions thus appear to be energetically strongly favored. This step morphology is illustrated in the top panel of fig. 2. From the FWHM at anti-phase conditions, an average step-to-step distance of 120 Å is estimated. This type of step morphology is in agreement with that found on other II-VI-(001) surfaces (HgTe [13], CdTe [14]) and is thus typical for these.

Similar to the (1×1) spots, the superstructure spots $(\pm\frac{1}{2}, \pm\frac{1}{2})$ are broadened along the [100] and the [010] direction due to steps (figs. 1(a) and (b)). But in contrast to the (1×1) spots, we find an *alternating* broadening along *either* the [100] or the [010] direction. This important observation is more clearly seen in figs. 1(c) and (d). It leads to an only *twofold* symmetry of the superstructure spots, in contrast to the *fourfold* symmetry of the (1×1) spots at anti-phase conditions. As a consequence, the LEED patterns show an alternating radial and azimuthal broadening of the superstructure spots as a function of energy as can be seen by comparing figs. 1(a) and (b). This hitherto not reported diffraction feature is a consequence of the specific step vectors on this surface. In other words, the step vectors are such that (for a specific superstructure spot and energy) a destructive interference occurs *either* at the [100] or at the [010] oriented steps, but not at both of them simultaneously, since this would result in a broadening with fourfold symmetry.

How can one determine these step vectors? The most convenient coordinate system for this purpose is given by the $[1\bar{1}0]$, $[110]$, and the $[001]$ directions and the lattice constant of the

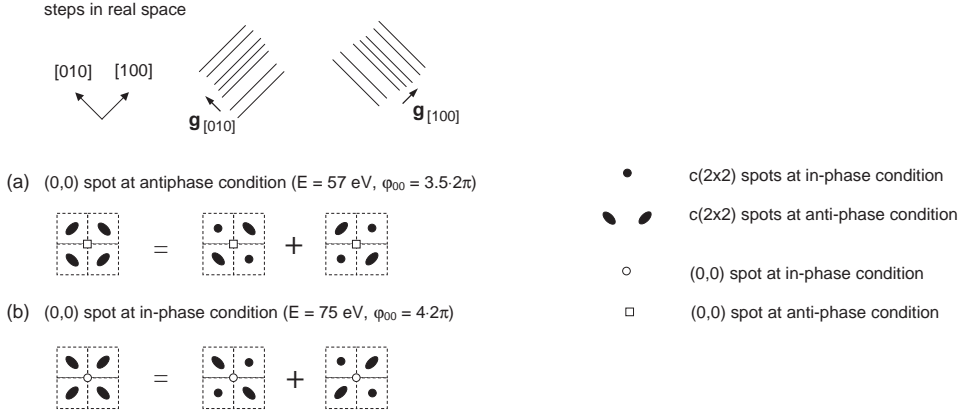


Fig. 2 – Schematic diagram of the steps in real space (at the top) and of the LEED patterns of fig. 1, illustrating the incoherent superposition of the spots broadened by the destructive interference at the steps along the [010] or [100] directions. Note that at the anti-phase condition for the (0, 0) spot (see (a)) only two of the four superstructure spots belonging to the $\mathbf{g}_{[010]}$ steps are also in anti-phase condition and hence elongated (middle column), while the other two superstructure spots are in anti-phase condition for the $\mathbf{g}_{[100]}$ steps (right column). In case (b) (in-phase condition for (0, 0) spot) the other two superstructure spots are in anti-phase condition and hence elongated in each case.

(001) surface ($a/\sqrt{2}$) as the length of the unit vector. (The [001] direction is perpendicular to the surface.) The step vectors of an *unreconstructed* (1×1) zinblende surface are

$$\mathbf{g}_{[100]} = \left(\frac{1}{2}, \frac{1}{2}, \pm \frac{1}{\sqrt{2}} \right), \tag{2a}$$

$$\mathbf{g}_{[010]} = \left(\frac{1}{2}, -\frac{1}{2}, \pm \frac{1}{\sqrt{2}} \right). \tag{2b}$$

These two step vectors are illustrated in fig. 3. The “ \pm ” signs in eqs. (2a) and (2b) refer to ascending and descending steps, respectively. The two step vectors transform into each other by a reflection at the $[1\bar{1}0]$ axis and are thus equivalent by symmetry.

For the $c(2 \times 2)$ *reconstructed* surface, *two* additional step vectors are possible, due to the existence of *two* degenerate $c(2 \times 2)$ domains, which are—in principle—possible on any terrace. This leads to a total of four step vectors. The additional two step vectors ($\mathbf{g}'_{[100]}$, $\mathbf{g}'_{[010]}$) can be generated by adding a relative displacement vector between the two $c(2 \times 2)$ domains to $\mathbf{g}_{[100]}$ and $\mathbf{g}_{[010]}$:

$$\mathbf{g}'_{[100]} = \left(\frac{1}{2}, \frac{1}{2} + 1, \pm \frac{1}{\sqrt{2}} \right), \tag{2c}$$

$$\mathbf{g}'_{[010]} = \left(\frac{1}{2}, -\frac{1}{2} - 1, \pm \frac{1}{\sqrt{2}} \right). \tag{2d}$$

In the corresponding reciprocal coordinate system, the \mathbf{k} -vectors of the first-order superstructure spots are given as $\mathbf{k}_{(\pm\frac{1}{2}, \pm\frac{1}{2})} = 2\pi \cdot (\pm\frac{1}{2}, \pm\frac{1}{2}, \mathbf{k}_\perp)$. From eqs. (1) and (2a)-(2d), the respective phase differences (φ) can be calculated. The important finding is that the step vectors $\mathbf{g}_{[100]}$ and $\mathbf{g}'_{[010]}$ belonging to steps of different orientation (or $\mathbf{g}_{[010]}$ and $\mathbf{g}'_{[100]}$, respectively) lead to the same φ values (mod (2π)), *i.e.* $\mathbf{k}_{(\pm\frac{1}{2}, \pm\frac{1}{2})} \cdot \mathbf{g}_{[100]} = \mathbf{k}_{(\pm\frac{1}{2}, \pm\frac{1}{2})} \cdot \mathbf{g}'_{[010]}$, and

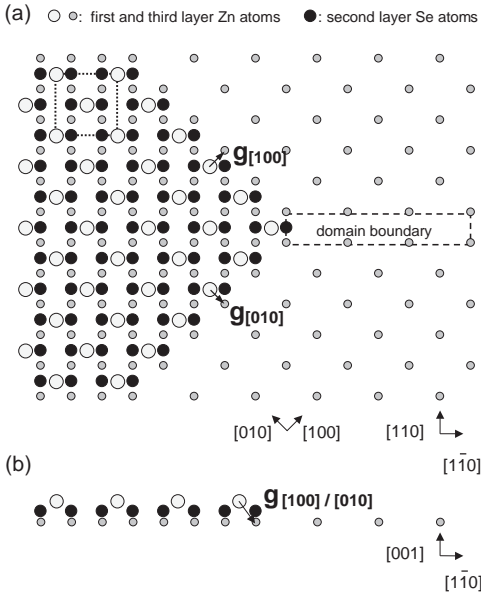


Fig. 3

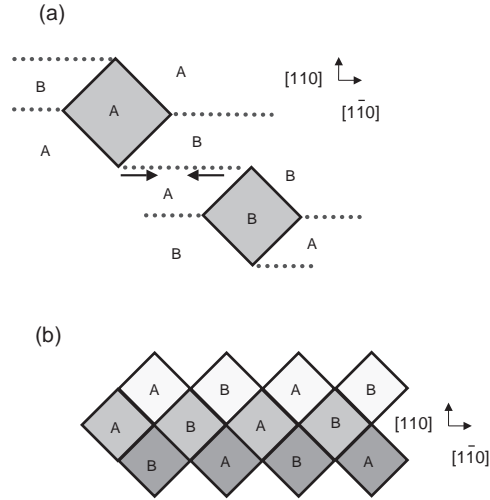


Fig. 4

Fig. 3 – Schematic hard-sphere model of a 2D island corner on the $c(2 \times 2)$ reconstructed ZnSe(001) surface with step vectors $\mathbf{g}_{[100]}$ and $\mathbf{g}_{[010]}$, respectively: (a) top view and (b) side view. The model demonstrates that the steps induce an anti-phase boundary with a local (2×1) reconstruction along the $[1\bar{1}0]$ direction on the lower terrace. The dotted square indicates the $c(2 \times 2)$ surface unit cell. Please note that this hard-sphere model is based on ideal bulk positions of the atoms and that significant displacement from these occur for the true reconstruction [10].

Fig. 4 – (a) Schematic drawing of two islands and of the induced anti-phase boundaries (dotted lines) between them. The two degenerate $c(2 \times 2)$ domains are marked by “A” and “B”. The arrows indicate the attractive force between the island corners mediated by the anti-phase boundary. (b) Schematic drawing of a vicinal (001) surface (surface normal tilted towards $[110]$, A-type) with a “checkerboard” arrangement of square-like terraces. The different gray shades correspond to different height levels.

$\mathbf{k}_{(\pm\frac{1}{2}, \pm\frac{1}{2})} \cdot \mathbf{g}_{[010]} = \mathbf{k}_{(\pm\frac{1}{2}, \pm\frac{1}{2})} \cdot \mathbf{g}'_{[100]}$. This is a consequence of the geometric structure of the steps and of the $c(2 \times 2)$ superstructure.

The consequence for the interpretation of the LEED patterns is the following: If all four step vectors were present on the surface, destructive interference from surface regions with $[100]$ and regions with $[010]$ oriented steps would occur simultaneously (at the same energy) and cause a broadening of the superstructure spots with fourfold symmetry. Since this is *not* observed, one must conclude that *only one of the two step vector pairs* ($\mathbf{g}_{[100]}, \mathbf{g}_{[010]}$) *or* ($\mathbf{g}'_{[100]}, \mathbf{g}'_{[010]}$) *is present on the surface, but not both*. This is consistent with the LEED pattern, since the phase differences related to $\mathbf{g}_{[100]}$ and $\mathbf{g}_{[010]}$ (or $\mathbf{g}'_{[100]}$ and $\mathbf{g}'_{[010]}$) differ by π . It is also consistent with the *either radial or azimuthal* broadening of the superstructure spots as a function of energy, as schematically illustrated in fig. 2 (lower part, for further explanation see the caption). From the direction of the broadening at a specific energy we further derive that only the step vector pair $\mathbf{g}_{[100]}, \mathbf{g}_{[010]}$ is realized. Moreover, the step vectors also explain the opposite broadening of the $(0, 0)$ spot in comparison with the first-order (1×1) spots (see figs. 1(a) and (b)), because they cause an additional phase difference of π for the first-order (1×1) spots relative to the $(0, 0)$ spot.

In essence, the occurrence of one specific step vector for each type of steps means that a $c(2 \times 2)$ domain on the upper terrace of a step determines the position of the $c(2 \times 2)$ domain on the lower terrace. Thus the $c(2 \times 2)$ domains are strictly *correlated* across the surface steps. Such a situation has been observed for chemisorbed adsorbates on metal surfaces, and appears to be related to a strong substrate reconstruction which mediates the lateral interaction across the steps [12]. Such a scenario is very conceivable here, too [10, 15, 16].

An interesting situation now occurs at the *intersection points* of [100] and [010] oriented steps, *i.e.*, at corners of 2D islands or kinks at rough step trains. The reason is that the two step vectors differ by a vector $\mathbf{g}_{[100]} - \mathbf{g}_{[010]} = (0, 1, 0)$, which is *incompatible* with the $c(2 \times 2)$ mesh. This causes the formation of an *anti-phase boundary* in the $c(2 \times 2)$ superstructure, either on the upper terrace (island) or on the lower terrace. From energetic arguments [6], a straight anti-phase boundary with a local (2×1) reconstruction running along the $[\bar{1}10]$ direction is favorable. This situation is illustrated in fig. 3. As a consequence, on a multilevel surface with [010] and [100] oriented steps an anti-phase boundary will nucleate at each intersection point. This is illustrated in fig. 4(a). The anti-phase boundaries cause an electron energy independent broadening of the LEED superstructure spots along the [110] direction, which is the reason why the elongation of the superstructure spots in figs. 1(c) and (d) (due to steps and anti-phase boundaries) is slightly rotated towards the [110] direction ($\sim 10^\circ$).

Unfortunately, scanning-tunneling-microscopy (STM) or atomic-force-microscopy data of the ZnSe(001) surface with atomic resolution is not available yet. However, this type of anti-phase boundaries, originating from the corners of 2D islands (as illustrated in fig. 4(a)), were observed in atomically resolved STM data of the $c(2 \times 2)$ CdTe(001) surface by Martrou *et al.* [14]. Since the $c(2 \times 2)$ reconstructions of the ZnSe and the CdTe(001) surfaces are very similar [6, 10, 16], we can take this as an additional support for our model.

The above finding leads to a further conclusion. Evidently, the existence of such anti-phase boundaries adds a non-local contribution to the step energies. In first order one may estimate the energy of an anti-phase boundary to be proportional to its length and the energetic difference between the local (2×1) reconstruction at the anti-phase boundary and the ideal $c(2 \times 2)$ surface reconstruction, which is of the order of 0.02–0.05 eV per (1×1) unit cell [6]. A likely situation is that an anti-phase boundary connects two step intersection points (as illustrated in fig. 4(a)). Since the energy of the anti-phase boundary is proportional to its length, it thus creates an attractive interaction between the two intersection points.

A remarkable consequence of these anti-phase boundaries is that they support surface morphologies which reduce or even avoid the formation such anti-phase boundaries. For instance, a vicinal ZnSe(001) or CdTe(001) surface tilted towards the [110] direction (A-type) can be expected to self-organize with a checkerboard-like arrangement of nano-terraces as illustrated in fig. 4(b). By merging of two step intersection points into *step crossing sites* [17], there are no anti-phase boundaries present for this particular surface morphology. Indeed, such a checkerboard surface morphology was observed for a vicinal (A-type) CdTe(001) surface by STM [18]. The authors of ref. [18] explained this morphology by the presence of long-range electrostatic interactions between dissymmetric step edges. In the framework of the present model, a complementary explanation is that this step morphology is energetically favored, since it systematically avoids the formation of anti-phase boundaries. We expect this mechanism to be important for other systems with similar structural constraints, too. Especially, it is predicted that under suitable preparation conditions a checkerboard morphology is formed on a vicinal ZnSe(001) surface. A recently found example is the (2×1) -reconstructed Au(110) surface [17], albeit the material constants and the geometric structure are considerably different to the polar semiconductor surfaces considered here.

In summary, we find that the steps on the sputter-annealed ZnSe(001)- $c(2 \times 2)$ surfaces are

aligned parallel to the [010] and [100] directions, and that the $c(2 \times 2)$ superstructure domains are correlated across these steps. As a consequence, step intersection points lead to $c(2 \times 2)$ anti-phase boundaries along the $[1\bar{1}0]$ direction, causing a reconstruction-induced, non-local energy contribution at kink sites or island corners. This mechanism influences the surface morphology. Quite in general, such step-induced anti-phase boundaries can be anticipated in all cases where a correlation of the superstructure across two types of (non-parallel) steps is present. Thus this mechanism is relevant not only for the explanation of the morphologies of polar II-VI semiconductor surfaces, but also —possibly in a modified form— for many other surfaces.

* * *

We thank J. NÜRNBERGER and C. SCHUMACHER for the preparation of the ZnSe samples and Drs. C. HESKE and CH. KUMPF for critical comments on the manuscript. This work was supported by the Deutsche Forschungsgemeinschaft within the SFB 410. One of us (ZHC) thanks the Volkswagen-Stiftung for financial support.

REFERENCES

- [1] AVERY A. R., GORINGE C. M., HOLMES D. M., SUDIJONO J. L. and JONES T. S., *Phys. Rev. Lett.*, **76** (1996) 3344.
- [2] ZHANG Q.-M., ROLAND C., BOGUSLAWSKI P. and BERNHOLC J., *Phys. Rev. Lett.*, **75** (1995) 101.
- [3] PEARSON C., BOROVSKY B., KRUEGER M., CURTIS R. and GANZ E., *Phys. Rev. Lett.*, **74** (1995) 2710.
- [4] MO Y.-W., SWARTZENTRUBER B. S., KARIOTIS R., WEBB M. B. and LAGALLY M. G., *Phys. Rev. Lett.*, **63** (1989) 2393.
- [5] PASHLEY M. D., HABERERN K. W. and GAINES J. M., *Appl. Phys. Lett.*, **58** (1991) 406; *Phys. Rev. B*, **40** (1989) 10481.
- [6] PARK C. H. and CHADI D. J., *Phys. Rev. B*, **49** (1994) 16467; GARCÍA A. and NORTHRUP J. E., *J. Vac. Sci. Technol. B*, **12** (1994) 2678.
- [7] CHEN W., KAHN A., SOUKIASSIAN P., MANGAT P. S., GAINES J., PONZONI C. and OLEGO D., *Phys. Rev. B*, **49** (1994) 10790.
- [8] CHEN Z. H., PhD Thesis, Universität Würzburg, Würzburg, Germany (1999).
- [9] OHTAKE A., HANADA T., YASUDA T., ARAI K. and YAO T., *Phys. Rev. B*, **60** (1999) 8326.
- [10] WEIGAND W., MÜLLER A., BUNK O., JOHNSON R. L., BACH P., SCHALLENBERG T., FASCHINGER W., MOLENKAMP L., KUMPF C. and UMBACH E., to be published.
- [11] HENZLER M., in *Electron Spectroscopy for Surface Analysis*, edited by IBACH H. (Springer-Verlag, Berlin) 1977, p. 117.
- [12] SOKOLOWSKI M., PFNÜR H. and LINDROOS M., *Surf. Sci.*, **278** (1992) 87.
- [13] OEHLING S., EHINGER M., GERHARD T., BECKER C. R., LANDWEHR G., SCHNEIDER M., EICH D., NEUREITER H., FINK R., SOKOLOWSKI M. and UMBACH E., *Appl. Phys. Lett.*, **73** (1998) 3205.
- [14] MARTROU D., EYMERY J., GENTILE P. and MAGNEA N., *J. Cryst. Growth*, **184/185** (1998) 203.
- [15] VERON M. B., SAUVAGE-SIMKIN M., ETGENS V. H., TATARENKO S., VAN DER VEGT H. A. and FERRER S., *Appl. Phys. Lett.*, **67** (1995) 3957.
- [16] GUNDEL S., FLESZAR A., FASCHINGER W. and HANKE W., *Phys. Rev. B*, **59** (1999) 15261.
- [17] ROST M. J., VAN GASTEL R. and FRENKEN J. W. M., *Phys. Rev. Lett.*, **84** (2000) 1966.
- [18] MARTROU D., EYMERY J. and MAGNEA N., *Phys. Rev. Lett.*, **83** (1999) 2366.